doi:10.1111/j.1365-2591.2008.01505.x

Finite element analysis of the effects of three preparation techniques on stresses within roots having curved canals

R. Cheng[1], X.-D. Zhou[1], Z. Liu[2], H. Yang[1], Q.-H. Gao[1] & T. Hu[1]

[1]State Key Laboratory of Oral Diseases; and [2]Laboratory of Biomechanical Engineering, Sichuan University, Chengdu, China

Abstract

Cheng R, Zhou X-D, Liu Z, Yang H, Gao Q-H, Hu T. Finite element analysis of the effects of three preparation techniques on stresses within roots having curved canals. *International Endodontic Journal*, **42**, 220–226, 2009.

Aim To compare stress distribution within roots having curved canals prepared by three preparation techniques when subjected to occlusal loads and condensation loads as a consequence of different filling techniques.

Methodology Three preparation techniques (crown-down, step-back and reverse-flaring) were compared by finite element analysis (FEA). Based on an established FEA model within curved canal, three modified models prepared by different preparation techniques were established by replacing original canal with prepared ones. FEA was performed to investigate the stress distribution under occlusal forces, which were simulated by loads of 500 N in four directions (buccal, lingual, mesial and distal), at 0 (vertical), 30, 45 and 60° to the longitudinal axis of the tooth. In addition, vertical and lateral condensation processes at the curvature were simulated to determine the influence of different canal filling techniques on stress distribution.

Results When the occlusal and the filling loads were applied, stress distribution around the curvature and the orifice had little change on the three modified prepared models. The reverse-flaring technique resulted in the least stress with the lateral condensation process. In the case of vertical condensation, the maximum von Mises stress (46.205 MPa) occurred near the loading site. The model also revealed a tendency for stress concentration (30.635 MPa) just below the compacting level.

Conclusions The study confirms that appropriate canal preparation techniques in simulated curved canals have little influence on stress distribution around the curvature or the orifice. However, vertical compaction induced high stress in the region just below the loading site.

Keywords: crown-down technique, finite element analysis, reverse-flaring technique, simulated canals, step-back technique.

Received 2 July 2007; accepted 18 October 2008

Introduction

Based on the properties of different material, finite element analysis (FEA) is used to determine the distribution of stress and strain when a structure is subjected to force. FEA can be adapted for use in the analysis of stresses that occur during compaction of filling material and occlusal procedures. For example, the effects of rotary NiTi and hand preparation were examined by FEA, with the results demonstrating that susceptibility to root fracture was reduced when the canal was smooth and round (Sathorn *et al.* 2005a). Other factors, such as dentine thickness (Lertchirakarn *et al.* 2003b, Sathorn *et al.* 2005b), and internal and external root morphology (Lertchirakarn *et al.* 2003a) could also potentially influence fracture susceptibility of roots.

Recently, high-resolution microfocus computed tomography (CT) has been used successfully in

Correspondence: Dr Tao Hu, State Key Laboratory of Oral Diseases, Sichuan University, 14# 3rd section, Renmin South Road, Chengdu 610041, China (Tel.: 086 028 85502415; fax: 86 28 85582167; e-mail: acomnet@263.com).

endodontics, especially when measuring the dimensions of canal system for use in FEA. In previous studies (Hubscher *et al.* 2003, Peters *et al.* 2003), microfocus CT produced valid root canal details in three dimensions, providing a method of estimating canal preparation techniques. Using microfocus CT, a precise FEA model of a curved canal was established (Cheng *et al.* 2007). To make the model repeatable and comparable, simulated curved canals with uniform shape were selected as prototype canals, and a suitable extracted single-root tooth was chosen as the outline.

This study, based on the FEA model (Cheng *et al.* 2007), aimed at showing the stress distribution on endodontically treated teeth with curved canals under various loads and at determining the differences between three preparation techniques. Subsequently, vertical and lateral compaction loads during filling were simulated and estimated by FEA.

Materials and methods

Instrumentation procedure

Three simulated canals (Dentsply Maillefer, Ballaigues, Switzerland) were selected randomly and fixed rigidly on a horizontal table. All subsequent procedures were undertaken by the same person.

Before use, stainless steel endodontic (SS) files (Dentsply Maillefer) for step-back technique and reverse-flaring technique were curved by a flexobend device (Dentsply Maillefer) to a curvature of approximate 30°. A precurved size-10 file was placed into the canal to its end-point. The working length (WL) was set 0.5-mm short of this length. Then, the canals were prepared as follows.

Sample 1: crown-down technique
The WL was 16.8 mm. ProTaper instruments were used according to the manufacturer's instructions as follows: S1 (6 mm), Sx (8 mm), S1 (16.8 mm), S2 (16.8 mm), F1 (16.8 mm) and F2 (16.8 mm). Finally, a size-25 file was placed at the WL and a 'snug' fit achieved. Copious irrigation with 1.0% NaOCl was used throughout the procedure.

Sample 2: step-back technique
A size-10 file and size-15 file could reach the WL (16.7 mm) without preparation. Then, using serial step-back preparation, the apical region was enlarged to size-25 at full WL. To create a flared shape each instrument beyond size-25 was inserted 1 mm short of the length of previous instrument up to size-40. Irrigation with 1.0% NaOCl was used throughout the preparation.

Sample 3: reverse-flaring technique (Yang et al. 2004)
First, size-10 and size-15 SS files were used to reach the WL (16.5 mm). The coronal 4 mm of the canal was initially prepared using a size-40 SS file. The canal preparation progressed in a step-down fashion in 3 mm increments with each smaller file size, down to a size-30 file. The apical region was then prepared according to the step-back technique to accept a size-25 file at the WL. Copious irrigation with 1.0% NaOCl was used throughout the procedure.

Development of finite element models

A three-dimensional FEA model within a curved canal was established by integrating a simulated canal and a natural tooth (Cheng *et al.* 2007). As judged by direct vision and radiography, a mandibular incisor with a canal similar in shape to the simulated canal was selected. The incisor was fixed with wax to maintain its position so that its curvature was parallel to that of the simulated canal. A micro-focus CT scanner (made by the Institute of Applied Electronics, China Academy of Engineering Physics, Mianyang, China) was used to scan the above models. The data were reconstructed to obtain a canal and a tooth model separately. After integration and modification, a final three-dimensional model with a smooth surface and a mostly centred canal was established.

Using clinical guidelines, the model was altered to accommodate canal preparation. An opening was set in the middle of the lingual fossa, with its end connected to the orifice of the canal. The canal was filled with gutta-percha from the apex to root canal orifice, with 1 mm of zinc phosphate cement placed coronally with amalgam on the surface. The thin cementum was neglected and the wall of the root was assumed to be dentine only. A periodontal ligament (PDL) was modelled as a 250-μm-thick shell surrounding the root and finished 1.5 mm apical to the cementoenamel junction. A cube of alveolar bone was modelled around the PDL. (Table 1) lists several typical tissue properties from the literature (Telli *et al.*1999).

Based on this model, three postoperative models were established by replacing the original canal. All the simulated canals were placed at the same level before

Table 1 Material properties

Material	Young's modulus (N mm^{-2})	Poisson's ratio
Enamel	8.41×10^4	0.300
Dentine	2.00×10^4	0.310
Periodontal ligament	5.00×10^1	0.490
Alveolar bone	1.40×10^4	0.150
Cold gutta-percha	3.00×10^2	0.485
Warm gutta-percha	3.00×10^0	0.485

scanning to eliminate horizontal differences. Postoperative canal images were rotated so that they were parallel to the original canal and then moved to the same position as the original image. During the procedure, rotating angle and moving distance were carefully measured to maintain precision. Figure 1 shows the three-dimensional models of the original canal and three prepared canals (CDT, SBT and RFT).

Boundary conditions and applied load

The tooth structure was loaded within its elastic range, and static linear analysis was performed. In this case, all loads were applied slowly until maximal values were attained. When the loads remained constant and the FEA model calculations had no variations, FEA was performed with the ABAQUS FEA software (ABAQUS6.5, ABAQUS Inc., Providence, RI, USA).

The model was loaded with a simulated 500 N force (Ichim *et al.* 2006) in four directions (buccal, lingual, mesial and distal), at 0 (vertical), 30, 45 and 60° to the longitudinal axis of the tooth. All the loads were applied onto the middle 2×2 mm^2 area of the incisal edge on the model.

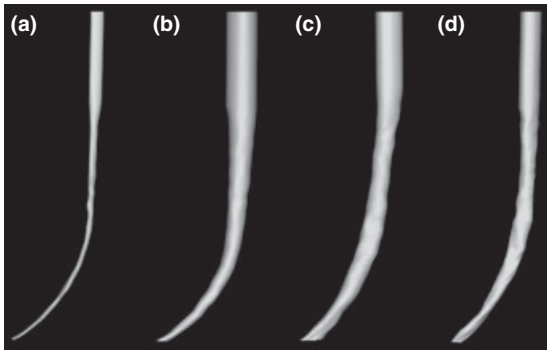

Figure 1 Three-dimensional model of four canals: (a) original model (O), (b) CDT, (c) SBT and (d) RFT.

To simulate compacting loads, a hypothetical force of 50 N (Rundquist & Versluis 2006) was applied. For lateral compactions, forces were loaded at four sites – buccal, lingual, mesial and distal (the curving direction was regarded as distal). This case described the cold gutta-percha material below the loading level. The space above it, without tight filling, was substituted by empty elements. The loading was limited to a selected spot, allowing for an appropriate simulation of a spreader inserting into the canal between the wall and the gutta-percha layer during the root filling process.

A vertical force was loaded onto gutta-percha to represent the pressure of a plugger during warm vertical compaction (WVC). The warm gutta-percha acted as an incompressible fluid, capable of pressing against the surface it touched but not able to distort in shear. Compacting was loaded at a selected level at the curvature (5 mm from the apex). In the first stage of the root filling process, the apical region of that canal was assumed to be filled with warm gutta-percha. Thus, the Young's modulus of the gutta-percha (Table 1) was different from that reported in a previous report (Telli *et al.*1999).

Results

Occlusal loads

Occlusal forces were loaded onto three postoperative models. The results demonstrated that stress distribution in these postoperative models were similar (Fig. 2a). Differences were not obvious at loads of 30 or 45°. When the loading angle increased to 60°, the three postoperative models had higher stress values than the original. The difference was also influenced by loading directions. In four directions, the distal load led to the highest stress values, and the buccal load had the least effect (Fig. 2b,c). Figure 3 showed the stresses of SBT model. Mesial (26.513 MPa) and distal loadings (27.398 MPa) led to higher stresses than buccal (18.745 MPa) and lingual loadings (20.911 MPa). The result remained the same in other postoperative models.

Condensation loads

Three postoperative models had similar stress distributions when condensation loads were applied. In the SBT model, vertical condensation loads resulted in much higher stress values than lateral forces, and the

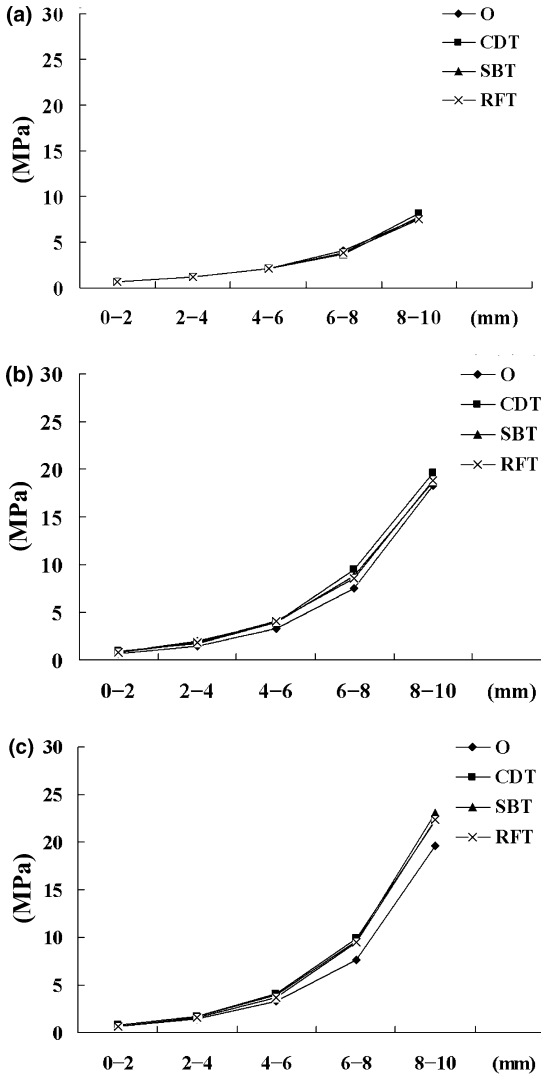

Figure 2 Maximal stresses of five apical regions under (a) vertical loading, (b) buccal load of 60°, (c) distal load of 60°.

maximal stress was 46.205 MPa (Figs 4 and 5). Especially in the region 2–4 mm from the apex (just below the curvature), the difference was obvious (30.653 MPa vs. 6.536 MPa.). The colour plot analysis gave an impression of stress concentration areas under vertical and lateral loads (Fig. 4). Vertical load induced an extended area of high stress below the loading level, while lateral loads led to a stress concentration area limited to the loading site.

When three prepared samples were compared, the maximal stress values for vertical loads showed little difference. However, under lateral loads, the CDT model had the highest stress (37.4 MPa) while the RFT model had the least stress (25.8 MPa) (Fig. 6a).

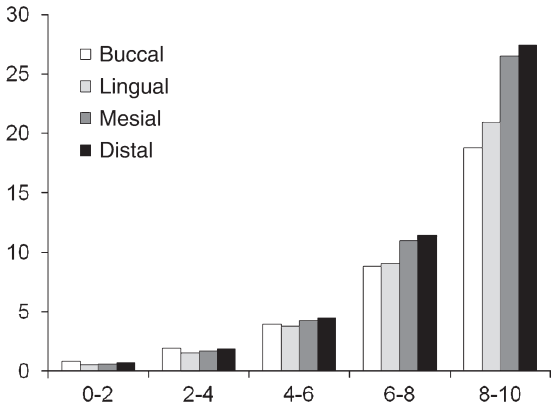

Figure 3 Maximal stresses of five apical regions under loads of 60° at four directions (SBT).

Discussion

In this study, the stress distribution within roots having curved canals when prepared by three preparation techniques was studied by FEA. Such a comparison might be useful for clinicians or manufacturers in selecting or designing instruments and techniques able to provide the best effects.

A previous study had shown that FEA was capable of evaluating stress distribution in roots with curved canals. In the present experiment, FEA models used in a previous study were modified (Versluis *et al.* 2006). Three postoperative models were established by replacing the inner canal, leaving the outline form unchanged to limit the interfering factors. For precise and credible modification, the new canals should be set at the same place as the original canal, which required that they had the same *X*-, *Y*- and *Z*-axis values. First, all the simulated canals were set at a horizontal level to eliminate differences in the *Y* axis. Next, they were rotated and shifted to have the same position in the *X*–*Z* plane. Finally, these canals were moved to the site of the original canal to replace it. This method establishes comparable and uniform FEA models within curved canals, but it only represents a simple condition. For example, simulated canals are so small that any technique will prepare them to a round cross section, a result not always presents in a real canal. In addition, dentine thickness in a simple root is relatively homogenous. By inserting a prepared canal from a plastic block into a model of a natural tooth, dentine thickness

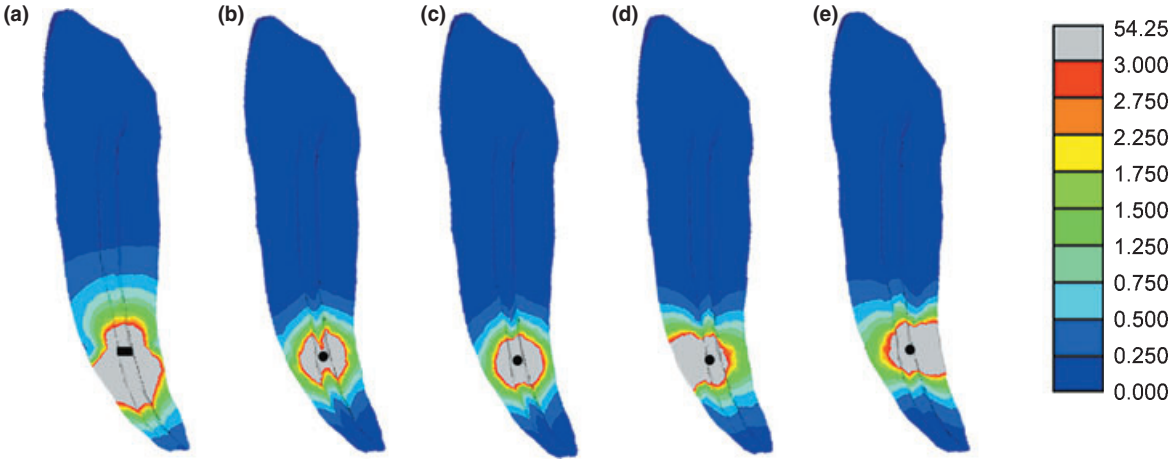

Figure 4 (a) Vertical compaction, (b) lateral compaction at the buccal point, (c) lateral compaction at the lingual point, (d) lateral compaction at the mesial point and (e) lateral compaction at the distal point. The black points on the figures represent the loading sites. Each colour represents a range of stress values (in MPa), corresponding to the scale.

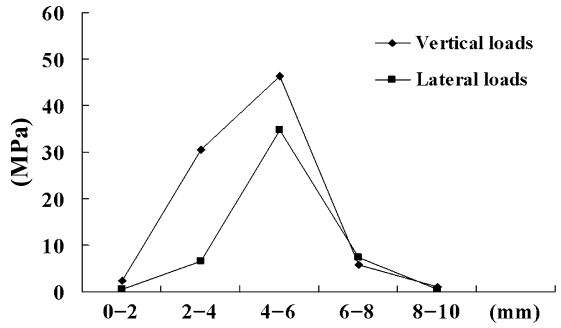

Figure 5 Maximal stresses at five apical regions under the vertical and lateral compactions of SBT.

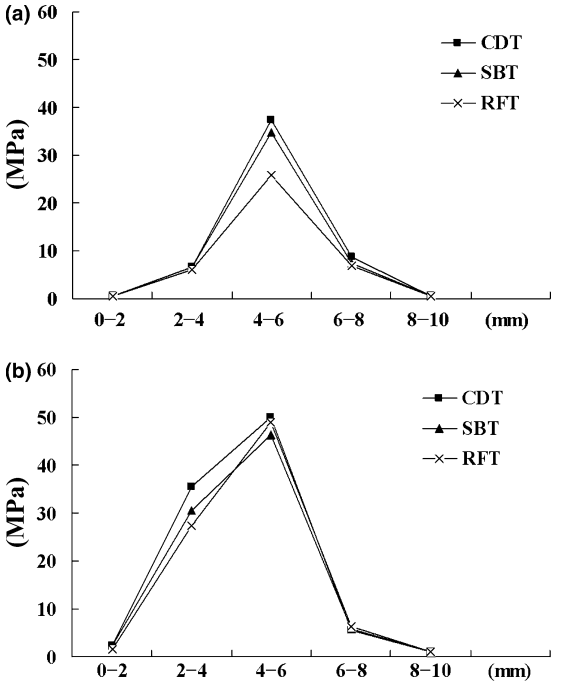

Figure 6 Maximal stresses at five apical regions in the three postoperative models: (a) under lateral compaction, (b) under vertical compaction.

is lost as a realistic factor. Furthermore, FEA results could only be evaluated as qualitative, because the results are theoretical. However, some other techniques such as strain-gauge techniques could validate root surface strain results obtained from FEA. The combination of modelling and strain-gauge measurement could yield more information regarding the mechanism of vertical root fracture (Lertchirakarn *et al.* 2003b).

In this study, all canals were prepared according to the manufacturer's instructions. Figure 1 provides a three-dimension model of the three canals, with a full-scale view. It was easier to see transportation at the apex and an overcutting at the curvature after SBT preparation, while CDT formed a better centred and continuously tapered canal. Compared with the other two techniques, the RFT specimen had two main features. First, the apical one-third of the RFT canal was similar to the SBT canal, but was smaller and had less transportation at the apex. The result may have something to do with the features of RFT. For example, in the apical region, RFT required fewer steps than SBT. As a result, excessive cutting was reduced. Second, the

upper two-thirds of the canal, though prepared according to a crown-down sequence, were not as large as the CDT model.

It was concluded that although the prepared canals varied in shape, little difference occurred in stress distribution around the root curvature and apex. The three preparation techniques had similar effects on simulated canals. After appropriate preparation, canals were enlarged and the stress increased to an extent below the tensile strength of dentine (50–100 MPa) (Craig *et al.* 1987, Sano *et al.* 1994). This finding was similar to that reported previously (Lam *et al.*2005).

In addition to the occlusal forces, lateral and vertical filling techniques were tested. The conditions were represented by a force of 50 N. Data were collected at the level of curvature, because it was a checking point for preparation and was accessible to a plugger. The results revealed that vertical compaction led to greater stress than lateral compaction. It coincided with the previous FEA of a maxillary canine (Telli and Gulkan 1998). In the case of the vertical condensation process, maximum von Mises stress (46.205 MPa) appeared at the loading level. The maximum stress value calculated in this study was close to the reported tensile strength of dentine (50–100 MPa). It was reported that a force of 10–30 N was safe for WVC (Telli & Gulkan 1998). These results suggest that excessive vertical compacting force (50 N) was likely to cause root fracture.

Vertical compaction also produced a stress concentration area below the compacting level (30.635 MPa). This might be attributed to the anatomy of curved canal because downward pressure was primarily passed down from the loading site to the curved part. Comparing the three techniques, RFT led to the least stress under lateral loads. As indicated above, RFT had combined features of both the CDT and SBT models, and as a result, it gave a thicker dentine wall around the curvature, reducing stress under different loadings.

Conclusions

The effect of three preparation techniques on stress distribution within roots having curved canals was studied. Three techniques (crown-down, step-back and reverse-flaring techniques) showed similar stress distribution in the lower part of FEA model when occlusal loads and condensation loads were applied. In the case of vertical condensation, maximum stress was close to the reported tensile strength of dentine. The warm vertical compaction technique was likely to create root fractures when excessive compaction forces (50 N) were loaded. The model also revealed a tendency for stress concentration below compacting level.

Acknowledgements

This study was supported by Program for Changjiang Scholars and Innovative Research Team in University, China (IRT0639) and the Program for New Century Excellent Talents in University (NCET-05-0790).

References

Cheng R, Zhou XD, Liu Z, Hu T (2007) Development of a finite element analysis model with curved canal and stress analysis. *Journal of Endodontics* **33**, 727–31.

Craig RG, O'Brien WJ, Powers JM (1987) *Dental Materials, Properties and Manipulation*, 4th edn. St Louis: C.V.Mosby.

Hubscher W, Barbakow F, Peters OA (2003) Root-canal preparation with FlexMaster: canal shapes analysed by micro-computed tomography. *International Endodontic Journal* **36**, 740–7.

Ichim I, Kuzmanovic DV, Love RM (2006) A finite element analysis of ferrule design on restoration resistance and distribution of stress within a root. *International Endodontic Journal* **39**, 443–52.

Lam PP, Palamara JE, Messer HH (2005) Fracture strength of tooth roots following canal preparation by hand and rotary instrumentation. *Journal of Endodontics* **31**, 529–32.

Lertchirakarn V, Palamara JE, Messer HH (2003a) Patterns of vertical root fracture: factors affecting stress distribution in the root canal. *Journal of Endodontics* **29**, 523–8.

Lertchirakarn V, Palamara JE, Messer HH (2003b) Finite element analysis and strain-gauge studies of vertical root fracture. *Journal of Endodontics* **29**, 529–34.

Peters OA, Peters CI, Schonenberger K, Barbakow F (2003) ProTaper rotary root canal preparation: effects of canal anatomy on final shape analysed by micro CT. *International Endodontic Journal* **36**, 86–92.

Rundquist BD, Versluis A (2006) How does canal taper affect root stresses? *International Endodontic Journal* **39**, 226–37.

Sano H, Ciucchi B, Matthews WG, Pashley DH (1994) Tensile properties of mineralized and demineralized human and bovine dentine. *Journal of Dental Research* **73**, 1205–11.

Sathorn C, Palamara JE, Messer HH (2005a) A comparison of the effects of two canal preparation techniques on root fracture susceptibility and fracture pattern. *Journal of Endodontics* **31**, 283–7.

Sathorn C, Palamara JE, Palamara D, Messer HH (2005b) Effect of root canal size and external root surface morphology on fracture susceptibility and pattern: a finite element analysis. *Journal of Endodontics* **31**, 288–92.

Telli C, Gulkan P (1998) Stress analysis during root canal filling by vertical and lateral condensation procedures: a

three-dimensional finite element model of a maxillary canine tooth. *British Dental Journal* **185**, 79–86.

Telli C, Gulkan P, Raab W (1999) Additional studies on the distribution of stresses during vertical compaction of gutta-percha in the root canal. *British Dental Journal* **187**, 32–7.

Versluis A, Messer HH, Pintado MR (2006) Changes in compaction stress distributions in roots resulting from canal preparation. *International Endodontic Journal* **39**, 931–9.

Yang JB, Liu TJ, Li JY (2004) Initial clinic research on curved canal preparation by reverse flaring technique. *West China Journal of Stomatology* **22**, 123–5.